International Journal of Engineering Science 90 (2015) 27–43

Contents lists available at ScienceDirect

International Journal of Engineering Science

journal homepage: www.elsevier.com/locate/ijengsci

Nonlinear effects in composite cylinders: relations and dependence on inhomogeneities

M.S. Wu *, Dong Wang

School of Mechanical and Aerospace Engineering, Nanyang Technological University, Singapore 639798

ARTICLE INFO

Article history:
Received 15 December 2014
Accepted 30 January 2015
Available online 21 February 2015

Keywords:
Poynting effect
Axial force–twist effect
Axial–torsional loading
Bilayered composites

ABSTRACT

The extension of a cylinder subjected to torsion was investigated by Poynting (1909) and the nonlinear phenomenon has since been called the Poynting effect. Under combined axial and torsional loading, the twist is also dependent on the axial loading as shown by Wang and Wu (2014a), who named this the axial force–twist effect. This paper investigates the relations between these effects in a bilayered cylindrical composite within the framework of second-order elasticity. The results show that: (1) either effect can be positive or negative, (2) there can only be three states, e.g., under tension–torsion either both effects are negative, or both positive, or if they differ in sign the Poynting effect must be positive and the axial force–twist effect must be negative, (3) certain logical relations between the effects exist, e.g., if under tension–torsion loading the Poynting effect is negative, the axial force–twist effect must be negative, (4) there exists a reduced elastic-geometric parameter between each effect and the associated applied loading, and (5) both effects are strong functions of the elastic and geometric inhomogeneities. These findings are significant for applications in regenerative medicine such as the design of replacement tissues.

1. Introduction

The extension of a cylinder under simple torsion was discovered by Poynting (1909) in the last century. This nonlinear phenomenon, accordingly named the Poynting effect, was experimentally observed for steel, copper and brass wires (Poynting, 1909, 1912) as well as for rubber-like solids (Lenoe, Heller, & Freudenthal, 1965). Nearly a century after its discovery, it was found that biopolymer gels sheared between parallel plates tend to draw the plates together, or they tend to develop a negative normal stress which may be comparable in magnitude to the shear stress (Janmey et al., 2007; Storm, Pastore, MacKintosh, Lubensky, & Janmey, 2005). This negative normal stress is akin to the axial contraction of a cylinder subjected to torsion, i.e., it corresponds to the negative or reverse Poynting effect. Experimental results supporting the occurrence of the negative effect in twisted fibers are available, e.g., stretched rabbit papillary muscles contracted in length when twisted (Horgan & Murphy, 2012).

To understand the Poynting effect, nonlinear elastic models have been used to investigate the torsion of bars and the shear of rectangular blocks. The strain energy functions can take various forms such as the neo-Hookean, Mooney-Rivlin, Ogden, and polynomial/exponential. Recent studies include (Destrade & Saccomandi, 2010; Horgan & Murphy, 2011, 2012; Mihai & Goriely, 2011, 2013; Wang & Wu, 2014a, 2014b; Wu & Kirchner, 2010;). Among these are the studies of

* Corresponding author. Tel.: +65 6790 5545.
E-mail addresses: mmswu@ntu.edu.sg (M.S. Wu), dwang2@e.ntu.edu.sg (D. Wang).

http://dx.doi.org/10.1016/j.ijengsci.2015.01.006
0020-7225/

the effect in transversely isotropic materials (Horgan & Murphy, 2011, 2012) and of bilayered composites (Wang & Wu, 2014a, 2014b). On the basis of second-order isotropic elasticity, Wang and Wu (2014a) demonstrated the possibility of both the Poynting effect under pure torsion and the "axial force–twist" effect under combined axial–torsional loading. The latter refers to a coupled nonlinear phenomenon in which the twist of a cylinder is affected by the axial loading, in addition to the applied torsion. The axial force–twist effect can also be either positive or negative. The positive effect means that the axial loading (either tension or compression) enhances the twist, while the negative effect means that it reduces the twist. The existence of such an effect is also suggested in the theoretical work of Zubov (2001), who referred this as the "inverse Poynting effect".

Nonlinear effects can play a pivotal role in the design considerations of artificial materials and in the understanding of biological functions, in view of much evidence that such functions can be significantly affected by mechanical stresses and deformations. For instance, the negative normal stress can influence the movement of mitochondria through the cytoskeleton of a narrow axon without distending the axon diameter, and it may also help in the compression of a fibrin gel at a wound site to a blood vessel due to shear flow in the vessel (Janmey et al., 2007). The interaction between surgical tool and tissue often occurs in the shearing mode, and the Poynting effect may result in normal forces that are larger or smaller than the human perception threshold for force discrimination (Misra, Ramesh, & Okamura, 2010). This has important implications for the design of surgical simulation systems that provide haptic feedback.

Besides nonlinearity and finite deformation, inhomogeneity, anisotropy and viscoelasticity may also play an important role in tissue mechanics. Inhomogeneity is given the primary focus in this work, as many biological and technological materials are composites. For instance, the aortic valve leaflet is composed of three morphologically distinct layers: fibrosa, spongiosa and ventricularis, and the development of novel heart valve therapies would depend on the synergistic mechanical behavior of the composite (Stella & Sacks, 2007). Another example is the development of polyelectrolyte multilayered capsules for the delivery of stem cells to induce bone formation in vivo (Facca et al., 2010). The multilayered structure enables the controlled delivery of different active molecules aimed at therapies such as gene and drug therapy.

Previous theoretical works have dealt largely with the Poynting effect in homogeneous materials. Wang and Wu (2014a) studied both the Poynting effect and the axial force–twist effect in a bilayered cylindrical composite. They showed that analytical expressions determining the sign and magnitude of the effects can be obtained for a bilayered cylindrical composite. However, the relations between these two effects, and their dependence on the elastic and geometric inhomogeneity between the layers, has not been explored. Elastic inhomogeneity refers to the dissimilarity between the layer elastic constants (both second- and third-order). Geometric inhomogeneity refers to the possible varying layer sizes: if r_1 and r_2 denote respectively the outer radii of the core and the outer layer of a bilayered cylinder, then $r_1 = 0$ and $r_1 = r_2$ both denote homogeneous cylinders while the ratio r_1/r_2 would serve as a measure of geometric inhomogeneity. This paper attempts to demonstrate that certain universal relations can be obtained for the Poynting and the axial force–twist effect of homogeneous, bilayered as well as hollow cylinders. Furthermore, it is shown that these effects are effectively captured by single parameters which are special combinations of the elastic and geometric parameters. The size dependence of these effects is also revealed in the analytical expressions. Investigation is carried out to show numerically how these effects depend on the elastic and geometric inhomogeneities.

This paper is organized in the following manner. A brief recapitulation of the second-order elastic model is first presented in Section 2, which incorporates analytical results for characterizing the Poynting effect and the axial force–twist effect in a bilayered cylinder. In particular, a universal relation between the two effects is demonstrated. The dependence of these effects on the elastic and geometric inhomogeneities is then presented in some detail in Section 3, highlighting the controllability of both the magnitude and sign of the effects. Further discussion follows in Section 4, and the paper concludes with a summary in Section 5.

2. Analytical expressions for the Poynting and axial force–twist effect

A summary of the formulation is given in Sections 2.1 and 2.2 below; the details are available in Wang and Wu (2014a). Based on the most general inhomogeneous case, further consideration of the following cases follows in Section 2.3: linearly inhomogeneous but nonlinearly homogeneous, linearly homogeneous but nonlinearly inhomogeneous, homogeneous, and hollow homogeneous. The emphasis of the current paper is on the relations between the Poynting effect and the axial force–twist effect for these various cases, as explained in Section 2.4.

2.1. Governing equations

The physical problem is that of a cylinder with two dissimilar concentric layers, as shown in Fig. 1. The core has a radius of r_1 while the outer layer has inner and outer radii of r_1 and r_2, respectively. The second-order elastic constants are the usual Lamé constants denoted by λ_i, μ_i, while the third-order ones by l_i, m_i and n_i, where $i = 1, 2$ denote the inner and outer layers, respectively. The bilayered cylinder is subjected to combined torsion T and axial loading P. The formulation below follows the perturbation procedure of Murnaghan (1951).

The final coordinates (ρ, ψ, ζ) of the particle of the cylinder whose initial coordinates being $(r,\ \theta, z)$ are assumed to be $(r + u_r,\ \theta + u_\theta/r,\ z + u_z)$, where the radial displacement $u_r = kF(r)$, the angular displacement $u_\theta/r = kG(z)$ and the axial

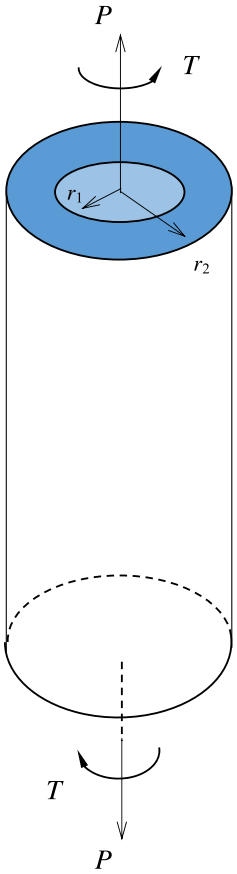

Fig. 1. A bilayered cylindrical composite, with surfaces located at the radial coordinates, $r = r_i, i = 1, 2$, under combined torsion T and axial loading P.

displacement $u_z = kH(z)$. The unknown displacements contain both parts: $F(r) = F_1(r) + kF_2(r), G(z) = G_1(z) + kG_2(z), H(z) = H_1(z) + kH_2(z)$. Here the marker k indicates the order of approximation of the theory. For second-order theory we retain terms up to k^2 in the formulation. The differentials of position vectors $\mathbf{a}$ and $\mathbf{x}(\mathbf{a})$ in the undeformed and deformed states can be written respectively as:

$$d\mathbf{a} = \begin{pmatrix} dr \\ rd\theta \\ dz \end{pmatrix}, \quad d\mathbf{x} = \begin{pmatrix} (1 + kF')dr \\ (r + kF)(d\theta + kG'dz) \\ (1 + kH')dz \end{pmatrix}, \tag{1}$$

where $F' = dF/dr = F_1'(r) + kF_2'(r), G' = dG/dz = G_1'(z) + kG_2'(z)$, and $H' = dH/dz = H_1'(z) + kH_2'(z)$. Accordingly the deformation gradient can be written as:

$$\mathbf{F} = \frac{d\mathbf{x}}{d\mathbf{a}} = \begin{pmatrix} 1 + kF' & 0 & 0 \\ 0 & 1 + \frac{kF}{r} & (r + kF)kG' \\ 0 & 0 & 1 + kH' \end{pmatrix}. \tag{2}$$

The governing equations are the equilibrium equations in terms of the first Piola–Kirchhoff stresses (relating forces in the current configuration to area vectors in the undeformed configuration). The equilibrium equations in cylindrical coordinates in terms of the first Piola–Kirchhoff stresses have been derived by Volokh (2006):

$$\frac{\partial T_{rr}}{\partial r} - T_{\theta r}\frac{\partial \psi}{\partial r} + \frac{T_{rr}}{r} + \frac{\partial T_{r\theta}}{r\partial \theta} - \frac{T_{\theta\theta}}{r}\frac{\partial \psi}{\partial \theta} + \frac{\partial T_{rz}}{\partial z} - T_{\theta z}\frac{\partial \psi}{\partial z} = 0, \tag{3}$$

$$T_{rr}\frac{\partial \psi}{\partial r} + \frac{\partial T_{\theta r}}{\partial r} + \frac{T_{r\theta}}{r}\frac{\partial \psi}{\partial \theta} + \frac{T_{\theta r}}{r} + \frac{\partial T_{\theta\theta}}{r\partial \theta} + \frac{\partial T_{\theta z}}{\partial z} + T_{rz}\frac{\partial \psi}{\partial z} = 0, \tag{4}$$

$$\frac{\partial T_{zr}}{\partial r}+\frac{T_{zr}}{r}+\frac{\partial T_{z\theta}}{r\partial\theta}+\frac{\partial T_{zz}}{\partial z}=0. \tag{5}$$

We note that the stress components such as T_{rr} should strictly be written as $T_{\rho r}$, which represents the stress along the ρ-direction in the deformed configuration with respect to the r-face in the undeformed configuration. The first Piola–Kirchhoff stress is defined as:

$$\mathbf{T}=\mathbf{F}\frac{\partial W}{\partial \mathbf{E}}, \tag{6}$$

where $\mathbf{E}$ is the Lagrangian strain. The energy density W of Murnaghan (1951) is adopted, with:

$$W=\frac{\lambda+2\mu}{2}J_1^2-2\mu J_2+\frac{l+2m}{3}J_1^3-2mJ_1J_2+nJ_3, \tag{7}$$

where λ and μ are the second-order and l,m,n the third-order elastic constants (the subscript i identifying the layers is dropped for convenience here), respectively, $\mathbf{I}$ is the identity, and J_1,J_2, and J_3 are the strain invariants of $\mathbf{E}$:

$$J_1=E_1+E_2+E_3,\quad J_2=E_1E_2+E_2E_3+E_3E_1,\quad J_3=E_1E_2E_3. \tag{8}$$

The Lagrangian strain is expressed in terms of the deformation gradient as:

$$\mathbf{E}=\frac{1}{2}(\mathbf{F}^*\mathbf{F}-\mathbf{I}), \tag{9}$$

where the asterisk in $\mathbf{F}^*$ denotes the transpose. At this point, it is useful to note that k in $\mathbf{F}$ as shown in Eq. 2 will lead to the presence of k^2 terms in $\mathbf{E}$ of Eq. (9) and to even higher order terms in J_2 and J_3 of Eq. (8). Hence, the first Piola–Kirchhoff stresses as defined in Eq. (6) will have k,k^2 and higher order terms. All terms of k^3 and higher orders will be discarded. It can also be seen that the stresses will therefore have the k and k^2 parts. The linear part will be labeled as T_{rr}^L,T_{zz}^L, etc., while the nonlinear parts as T_{rr}^{NL},T_{zz}^{NL}, etc.

Substituting the stresses into Eqs. (3)–(5) with $\partial\psi/\partial r=0,\partial T_{r\theta}/\partial\theta=0,\partial\psi/\partial\theta=1,\partial\psi/\partial z=kG'$ yields three first-order and three second-order equilibrium equations as distinguished by the k and k^2 multipliers:

$$k\left(\frac{F_1''(r)}{r}+\frac{F_1'(r)}{r}-\frac{F_1'(r)}{r^2}\right)=0, \tag{10}$$

$$kG_1'(z)=0, \tag{11}$$

$$kH_1''(z)=0, \tag{12}$$

$$\begin{aligned}k^2\{&-4(2l+2m+2\lambda+3\mu)F_1(r)^2+r^4(4m-3n+4\lambda-8\mu)G_1'(z)^2+r[-4(\lambda+2\mu)F_2(r)-4(2l+\lambda)F_1(r)H_1'(z)]\\&+4r^2[(2l+2m+2\lambda+3\mu)F_1'(r)^2+(\lambda+2\mu)F_2'(r)+(2l+\lambda)F_1'(r)H_1'(z)+(2l+\lambda)F_1(r)F_1''(r)]+4r^3[(2l+4m+3\lambda\\&+6\mu)F_1'(r)F_1''(r)+(2l+\lambda)H_1'(z)F_1''(r)+(\lambda+2\mu)F_2''(r)]\}=0,\end{aligned} \tag{13}$$

$$k^2\left\{(m+\lambda+3\mu)F_1(r)G_1''(z)+r\left[\frac{1}{2}(2m-n+2\lambda)F_1'(r)G_1''(z)+(m+\lambda+2\mu)H_1'(z)G_1''(z)+\mu G_2''(z)+(m+\lambda+2\mu)G_1'(z)H_1''(z)\right]\right\}=0, \tag{14}$$

$$k^2\{r^3(m+\lambda+2\mu)G_1'(z)G_1''(z)+(2l+\lambda)F_1(r)H_1''(z)+r[(2l+\lambda)F_1'(r)H_1''(z)+(2l+4m+3\lambda+6\mu)H_1'(z)H_1''(z)+(\lambda+2\mu)H_2''(z)]\}=0. \tag{15}$$

The unknown functions F_1,F_2,G_1,G_2,H_1 and H_2 related to the displacements in the bilayered cylinder can be solved from these equilibrium equations by using appropriate boundary conditions summarized in Section 2.2.

2.2. Boundary conditions

The following boundary conditions are applied to solve the problem. Since the layers must be explicitly considered, we introduce the notations λ_1, λ_2, etc. and $T_{rr}^{L(1)},T_{rr}^{L(2)}$, etc., with 1 and 2 denoting the layers.

(1) Load Boundary conditions:

(BC1) T_{rr}^L vanishes on the outer boundary $r=r_2$:

$$T_{rr}^{L(2)}(r=r_2)=0,\quad T_{rr}^{NL(2)}(r=r_2)=0. \tag{16}$$

(BC2) The summation of the axial forces acting at either end of the cylinder is $P\pi r_2^2$:

$$\int T_{zz}^{L(i)}(z=0,L)dA = P\pi r_2^2, \quad \int T_{zz}^{NL(i)}(z=0,L)dA = 0. \tag{17}$$

(BC3) The torsion applied to the cylinder is T:

$$\int T_{\theta z}^{L(i)} r dA = T, \quad \int T_{\theta z}^{NL(i)}(z=0,L) r dA = 0. \tag{18}$$

(2) Interface boundary conditions:

(BC4) Linear and nonlinear radial displacements are continuous across the interface $r = r_1$:

$$F_1^{(1)}(r=r_1) = F_1^{(2)}(r=r_1), \quad F_2^{(1)}(r=r_1) = F_2^{(2)}(r=r_1). \tag{19}$$

(BC5) Linear and nonlinear circumferential displacements are continuous across the interface:

$$G_1^{(1)}(r=r_1) = G_1^{(2)}(r=r_1), \quad G_2^{(1)}(r=r_1) = G_2^{(2)}(r=r_1). \tag{20}$$

(BC6) Linear and nonlinear axial displacements are continuous across the interface:

$$H_1^{(1)}(r=r_1) = H_1^{(2)}(r=r_1), \quad H_2^{(1)}(r=r_1) = H_2^{(2)}(r=r_1). \tag{21}$$

(BC7) Linear and nonlinear radial tractions T_{rr}^{L} are T_{rr}^{NL} continuous across the interface:

$$T_{rr}^{L(1)}(r=r_1) = T_{rr}^{L(2)}(r=r_1), \quad T_{rr}^{NL(1)}(r=r_1) = T_{rr}^{NL(2)}(r=r_1). \tag{22}$$

Using the above boundary conditions, both the linear and nonlinear displacements can be solved. Substituting the displacements into Eq. (6), the stress field can be obtained for each layer. Setting $T = 0$, the solutions for a bilayered cylinder under axial loading can be obtained. Similarly, the solutions for a bilayered cylinder under pure torsion can be obtained by setting $P = 0$.

2.3. Solutions

The results for the axial displacement (related to the Poynting effect) and for the circumferential displacement (related to the axial force–twist effect) are given below. Solutions not related to these effects are omitted.

The axial displacement $u_z(P,T)$ can be written as the simple additive sum of that due to P and T acting alone:

$$u_z(P,T) = u_z(P) + u_z(T), \tag{23}$$

where the axial displacement $u_z(T)$ can be written as:

$$u_z(T) = k^2 Dz. \tag{24}$$

The axial displacement $u_z(P)$ due to the axial loading P is omitted here. The parameter D is the Poynting effect coefficient for the bilayered cylinder, where:

$$D = C_D \frac{T^2}{4\pi^2}, \quad C_D = \frac{B}{M^2 C}, \tag{25}$$

and B, M, C are given later. Note that $u_z(T)$ is second-order only and hence the Poynting effect is a nonlinear phenomenon. The parameter C_D is a reduced coefficient of the elastic and geometric parameters of the two layers. It uniquely characterizes the quadratic relation between the Poynting effect and T.

The circumferential displacement $u_\theta(P,T)$ can be written as:

$$u_\theta(P,T) = u_\theta^L(P,T) + u_\theta^{NL}(P,T), \tag{26}$$

where the linear part $u_\theta^L(P,T)$ can be additively decomposed into the parts due to P and T acting alone: $u_\theta^L(P,T) = u_\theta^L(P) + u_\theta^L(T)$, with

$$u_\theta^L(P) = 0, \tag{27}$$

$$u_\theta^L(T) = k \frac{2T}{\pi\left(r_1^4\mu_1 - r_1^4\mu_2 + r_2^4\mu_2\right)} rz. \tag{28}$$

Eq. (27) simply states that a composite bar cannot twist under pure uniaxial loading. Eq. (28) gives the twist of the bar under pure torsion. Furthermore, the nonlinear part $u_\theta^{NL}(P,T)$ in Eq. (26) can be written as:

$$u_\theta^{NL}(P,T) = k^2 \frac{2T}{\pi\left(r_1^4\mu_1 - r_1^4\mu_2 + r_2^4\mu_2\right)} Hrz, \tag{29}$$

where H is dependent on P and is defined as the axial force–twist effect coefficient with the following form (omitting the marker k):

$$H = \frac{u_\theta^{NL}}{u_\theta^{L}} = C_H \frac{P}{4} r_2^2, \quad C_H = \frac{A}{MC}. \tag{30}$$

C_H is a reduced coefficient which characterizes the linear relation between H and P. It is noted that $u_\theta^{NL}(P,T)$ in Eq. (29) cannot be written as the sum of the parts due to P and T acting alone; P and T in this nonlinear circumferential displacement are multiplicatively coupled.

For the generally inhomogeneous bilayered composite, the elastic-geometric parameters A, B, C and M can be written as polynomials in r_1 and r_2 with the elastic constants of the two layers as coefficients. The reduced coefficients $C_D = B/M^2C$ in Eq. (25) and $C_H = A/MC$ in Eq. (30) have the following significance. The Poynting effect or the axial force–twist effect will be identical in sign and magnitude for all elastic and geometrical inhomogeneities provided the C_D or the C_H values for these different materials are the same. The constituent parameters A, B, C and M have not been investigated previously. The first parameter A is a sixth-order polynomial given by:

$$A = \alpha_1 r_1^6 + \alpha_2 r_1^4 r_2^2 + \alpha_3 r_1^2 r_2^4 + \alpha_4 r_2^6, \tag{31}$$

where

$$\alpha_1 = \big(n_2(\lambda_1 - \lambda_2) + n_1(-\lambda_1 + \lambda_2) - 2\big(2m_1 - 2m_2 + 3\lambda_1 - 3\lambda_2 + 4\mu_1 - 4\mu_2\big)(\mu_1 - \mu_2)\big)\mu_2, \tag{31a}$$

$$\begin{aligned}\alpha_2 = {} & -\lambda_2\big((n_1 - n_2)\lambda_1 + (4m_1 - 3n_2 + 6\lambda_1)\mu_1 + 8\mu_1^2\big) \\ & + \big(-2n_2\lambda_1 + n_2\lambda_2 + 6\lambda_1\lambda_2 - n_1(\lambda_1 + \lambda_2) - 2(2m_1 + 3\lambda_1 - 8\lambda_2)\mu_1 - 8\mu_1^2 + 4m_2(\lambda_1 + \mu_1)\big)\mu_2 \\ & + 2(-2m_1 + 2m_2 - 4\lambda_1 + 3\lambda_2)\mu_2^2 + 8\mu_2^3,\end{aligned} \tag{31b}$$

$$\alpha_3 = n_2\big(-2\lambda_2\mu_1 + (\lambda_1 + \lambda_2)\mu_2\big) + 2\mu_2\big(-2(m_2 + 4\lambda_2)\mu_1 + \big(2m_2 + 5\lambda_1 + 3\lambda_2 - 4\mu_1\big)\mu_2 + 4\mu_2^2\big), \tag{31c}$$

$$\alpha_4 = -\big(\lambda_1 + \mu_1 + \mu_2\big)\big(n_2\lambda_2 + 2\mu_2\big(2m_2 + 3\lambda_2 + 4\mu_2\big)\big). \tag{31d}$$

The second parameter B is also a sixth-order polynomial:

$$B = \beta_1 r_1^6 + \beta_2 r_1^4 r_2^2 + \beta_3 r_1^2 r_2^4 + \beta_4 r_2^6, \tag{32}$$

where

$$\beta_1 = \big(n_2(\lambda_1 - \lambda_2) + n_1(-\lambda_1 + \lambda_2) - 4\big(m_1 - m_2 + \lambda_1 - \lambda_2 + 2\mu_1 - 2\mu_2\big)(\mu_1 - \mu_2)\big)\mu_2, \tag{32a}$$

$$\begin{aligned}\beta_2 = {} & -\lambda_2\big(n_1\lambda_1 + 4\mu_1\big(m_1 + \lambda_1 + 2\mu_1\big) - n_2\big(\lambda_1 + 3\mu_1\big)\big) \\ & + \big(-2n_2\lambda_1 + n_2\lambda_2 + 4\lambda_1\lambda_2 - n_1(\lambda_1 + \lambda_2) - 4(m_1 + \lambda_1 - 5\lambda_2)\mu_1 - 8\mu_1^2 + 4m_2(\lambda_1 + \mu_1)\big)\mu_2 \\ & + 4(-m_1 + m_2 - 3\lambda_1 + \lambda_2)\mu_2^2 + 8\mu_2^3,\end{aligned} \tag{32b}$$

$$\beta_3 = n_2\big(-2\lambda_2\mu_1 + (\lambda_1 + \lambda_2)\mu_2\big) + 4\mu_2\big(-(m_2 + 5\lambda_2)\mu_1 + \big(m_2 + 4\lambda_1 + \lambda_2 - 2\mu_1\big)\mu_2 + 2\mu_2^2\big), \tag{32c}$$

$$\beta_4 = -\big(\lambda_1 + \mu_1 + \mu_2\big)\big(n_2\lambda_2 + 4\mu_2\big(m_2 + \lambda_2 + 2\mu_2\big)\big). \tag{32d}$$

The third parameter C is a quartic:

$$C = \gamma_1 r_1^4 + \gamma_2 r_1^2 r_2^2 + \gamma_3 r_2^4, \tag{33}$$

where

$$\gamma_1 = \big(3\lambda_1 - 3\lambda_2 + 2\mu_1 - 2\mu_2\big)(\mu_1 - \mu_2)\mu_2, \tag{33a}$$

$$\gamma_2 = \lambda_2\mu_1\big(3\lambda_1 + 2\mu_1\big) + \big(2\mu_1^2 + 3\lambda_1\big(-\lambda_2 + \mu_1\big)\big)\mu_2 + \big(\lambda_1 - 6\lambda_2 + 2\mu_1\big)\mu_2^2 - 4\mu_2^3, \tag{33b}$$

$$\gamma_3 = \mu_2\big(\lambda_1 + \mu_1 + \mu_2\big)\big(3\lambda_2 + 2\mu_2\big), \tag{33c}$$

Finally, M is also a quartic:

$$M = r_1^4(\mu_1 - \mu_2) + r_2^4\mu_2. \tag{34}$$

Among these inhomogeneous parameters, A and B are dependent on the elastic constants $\lambda_i, \mu_i, m_i, n_i, i = 1, 2$. The third-order elastic constants l_i do not appear for cylindrical symmetry. On the other hand, C and M depend only on λ_i, μ_i. It can be concluded that the inhomogeneity parameters are sextic and quartic polynomials in the radii with the combinations of elastic constants as coefficients.

We next consider special cases of the cylinder with various inhomogeneities, including (1) linear inhomogeneous but nonlinear homogeneous, (2) linear homogeneous but nonlinear inhomogeneous, (3) solid homogeneous, and (4) and hollow homogeneous.

(1) For a linear inhomogeneous but nonlinear homogeneous bilayered cylinder, i.e., $m_1 = m_2 = m, n_1 = n_2 = n$, the elastic coefficients in A, B and C reduce to:

$$\alpha_1 = -2(3\lambda_1 - 3\lambda_2 + 4\mu_1 - 4\mu_2)(\mu_1 - \mu_2)\mu_2, \tag{35a}$$

$$\alpha_2 = -4m\lambda_2\mu_1 + 3n\lambda_2\mu_1 - 6\lambda_1\lambda_2\mu_1 - 8\lambda_2\mu_1^2 + 4m\lambda_1\mu_2 - 3n\lambda_1\mu_2 + 6\lambda_1\lambda_2\mu_2 - 6\lambda_1\mu_1\mu_2 + 16\lambda_2\mu_1\mu_2 - 8\mu_1^2\mu_2 - 8\lambda_1\mu_2^2 + 6\lambda_2\mu_2^2 + 8\mu_2^3, \tag{35b}$$

$$\alpha_3 = 2\mu_2(-2m\mu_1 - 8\lambda_2\mu_1 + 2m\mu_2 + 5\lambda_1\mu_2 + 3\lambda_2\mu_2 - 4\mu_1\mu_2 + 4\mu_2^2) + n(\lambda_1\mu_2 + \lambda_2(-2\mu_1 + \mu_2)), \tag{35c}$$

$$\alpha_4 = -(\lambda_1 + \mu_1 + \mu_2)(n\lambda_2 + 2\mu_2(2m + 3\lambda_2 + 4\mu_2)), \tag{35d}$$

$$\beta_1 = -4(\lambda_1 - \lambda_2 + 2\mu_1 - 2\mu_2)(\mu_1 - \mu_2)\mu_2, \tag{36a}$$

$$\beta_2 = -4m\lambda_2\mu_1 + 3n\lambda_2\mu_1 - 4\lambda_1\lambda_2\mu_1 - 8\lambda_2\mu_1^2 + 4m\lambda_1\mu_2 - 3n\lambda_1\mu_2 + 4\lambda_1\lambda_2\mu_2 - 4\lambda_1\mu_1\mu_2 + 20\lambda_2\mu_1\mu_2 - 8\mu_1^2\mu_2 - 12\lambda_1\mu_2^2 + 4\lambda_2\mu_2^2 + 8\mu_2^3, \tag{36b}$$

$$\beta_3 = n(\lambda_1\mu_2 + \lambda_2(-2\mu_1 + \mu_2)) + 4\mu_2(\lambda_2(-5\mu_1 + \mu_2) + m(-\mu_1 + \mu_2) + 2\mu_2(2\lambda_1 - \mu_1 + \mu_2)), \tag{36c}$$

$$\beta_4 = -(\lambda_1 + \mu_1 + \mu_2)(n\lambda_2 + 4\mu_2(m + \lambda_2 + 2\mu_2)), \tag{36d}$$

$$\gamma_1 = (3\lambda_1 - 3\lambda_2 + 2\mu_1 - 2\mu_2)(\mu_1 - \mu_2)\mu_2, \tag{37a}$$

$$\gamma_2 = \lambda_1(3\lambda_2(\mu_1 - \mu_2) + \mu_2(3\mu_1 + \mu_2)) + 2(\lambda_2(\mu_1^2 - 3\mu_2^2) + \mu_2(\mu_1^2 + \mu_1\mu_2 - 2\mu_2^2)), \tag{37b}$$

$$\gamma_3 = \mu_2(\lambda_1 + \mu_1 + \mu_2)(3\lambda_2 + 2\mu_2). \tag{37c}$$

It can be seen that all the coefficients exist, but with α_2, α_3, α_4, β_2, β_3, β_4 dependent on both the second- and third-order elastic constants and the rest dependent on only the Lamé constants.

(2) For a linear homogeneous but nonlinear inhomogeneous bilayered cylinder, i.e., $\lambda_1 = \lambda_2 = \lambda, \mu_1 = \mu_2 = \mu$, the coefficients simplify to:

$$\alpha_1 = 0, \tag{38a}$$

$$\alpha_2 = -(\lambda + 2\mu)(n_1\lambda - n_2\lambda + 4(m_1 - m_2)\mu), \tag{38b}$$

$$\alpha_3 = 0, \tag{38c}$$

$$\alpha_4 = -(\lambda + 2\mu)(n_2\lambda + 2\mu(2m_2 + 3\lambda + 4\mu)), \tag{38d}$$

$$\beta_1 = 0, \tag{39a}$$

$$\beta_2 = -(\lambda + 2\mu)((n_1 - n_2)\lambda + 4(m_1 - m_2)\mu), \tag{39b}$$

$$\beta_3 = 0, \tag{39c}$$

$$\beta_4 = -(\lambda + 2\mu)(n_2\lambda + 4\mu(m_2 + \lambda + 2\mu)), \tag{39d}$$

$$\gamma_1 = 0, \tag{40a}$$

$$\gamma_2 = 0, \tag{40b}$$

$$\gamma_3 = \mu(\lambda + 2\mu)(3\lambda + 2\mu). \tag{40c}$$

It can be seen that α_1, α_3, β_1, β_3, γ_1, γ_2 are all zero. For the non-zero terms α_2, β_2 and γ_3, note that γ_3 depends only on the Lamé constants. Also, α_1, α_3, β_1, β_3, γ_1 and γ_2 can be regarded as linear inhomogeneity coefficients, because they disappear when the materials become linear homogeneous.

(3) For a homogeneous solid cylinder, i.e., $\lambda_1=\lambda_2=\lambda, \mu_1=\mu_2=\mu, m_1=m_2=m, n_1=n_2=n$, there are only three non-zero coefficients:

$$\alpha_1=0,\quad \alpha_2=0,\quad \alpha_3=0,\quad \alpha_4=-(\lambda+2\mu)(n\lambda+2\mu(2m+3\lambda+4\mu)), \tag{41a}$$

$$\beta_1=0,\quad \beta_2=0,\quad \beta_3=0,\quad \beta_4=-(\lambda+2\mu)(n\lambda+4\mu(m+\lambda+2\mu)), \tag{41b}$$

$$\gamma_1=0,\quad \gamma_2=0,\quad \gamma_3=\mu_1(\lambda+2\mu)(3\lambda+2\mu). \tag{41c}$$

The coefficients α_2 and β_2 become zero from Case (2) to Case (3). Thus they can be named as intrinsic inhomogeneity coefficients because they only disappear when the materials are both linear and nonlinear homogeneous. Finally, α_4, β_4 and γ_3 can be named as fundamental elastic coefficients, because they always exist whether the materials are homogeneous or inhomogeneous.

In summary, the inhomogeneity coefficients can be categorized as: (a) fundamental elastic coefficients: α_4, β_4 and γ_3, and (b) inhomogeneity elastic coefficients: α_1, α_2, α_3, β_1, β_2, β_3, γ_1 and γ_2, where α_1, α_3, β_1, β_3, γ_1 and γ_2 are linear inhomogeneity coefficients and α_2, β_2 are intrinsic inhomogeneity coefficients.

(4) For a hollow cylinder, i.e., $\lambda_1=0, \mu_1=0, m_1=0, n_1=0$, the coefficients in Eqs. (31)–(33) become:

$$\alpha_1=\alpha_4=-\alpha_2=-\alpha_3=-\mu_2\left(n_2\lambda_2+2\mu_2\left(2m_2+3\lambda_2+4\mu_2\right)\right), \tag{42}$$

$$\beta_1=\beta_4=-\beta_2=-\beta_3=-\mu_2\left(n_2\lambda_2+4\mu_2\left(m_2+\lambda_2+2\mu_2\right)\right), \tag{43}$$

$$\gamma_1=\gamma_3=-\gamma_2/2=\mu_2^2\left(3\lambda_2+2\mu_2\right), \tag{44}$$

From all the results presented in this section, it can be observed that the n is always associated with λ (whenever n appears, so does λ) whereas m is always associated with μ (whenever m appears, so does μ). The terms involving the third-order elastic constants m and n only exist in the following forms: $m\mu^2,\ m\lambda\mu,\ n\lambda^2,\ n\lambda\mu$. It can also be seen that λ^3 does not exist; the terms involving only second-order elastic constants are $\lambda\mu^2,\ \lambda^2\mu$ and μ^3. Because of the m-μ association, increasing m will automatically increase the influence of μ more than λ. In contrast, then-λ association means that increasing n will automatically increase the influence of λ more than μ.

The size dependence of the Poynting effect and the axial force–twist effect can be deduced from the expressions for u_z under torsion and u_θ^{NL} under axial–torsional loading. This is best inferred by considering a homogeneous cylinder of radius R, for which Eqs. (24) and (29) reduce to:

$$u_z=-k^2\frac{n\lambda+4\mu(m+\lambda+2\mu)}{4\pi^2R^6\mu^3(3\lambda+2\mu)}T^2z, \tag{45}$$

$$u_\theta^{NL}=-k^2\frac{n\lambda+2\mu(2m+3\lambda+4\mu)}{2\pi R^4\mu^3(3\lambda+2\mu)}PTrz. \tag{46}$$

It can be observed that the Poynting effect obeys an inverse sextic power dependence on R while the axial force–twist effect an inverse cubic dependence on R. Note that u_θ^{NL} is a function of r; the size effect is evaluated at $r=R$.

2.4. Relations between Poynting and axial force–twist effects

Consider a bilayered cylinder in the general case, with eight elastic constants and two radii. By using $r_1<r_2$, it can be proved that $M>0$, $C>0$ and $B-A=\xi>0$, where

$$\begin{aligned}\xi=2\big[&r_1^4r_2^2\lambda_1\lambda_2\mu_1+(r_2^6-r_1^4r_2^2)\lambda_1\lambda_2\mu_2+(r_1^6+r_1^4r_2^2)\lambda_1\mu_1\mu_2+(2r_1^4r_2^2-r_1^6-2r_1^2r_2^4+r_2^6)\lambda_2\mu_1\mu_2\\&+(3r_1^2r_2^4-2r_1^4r_2^2-r_1^6)\lambda_1\mu_2^2+(r_1^6-r_1^4r_2^2-r_1^2r_2^4+r_2^6)\lambda_2\mu_2^2\big]\end{aligned} \tag{47}$$

Thus, by Eqs. (25) and (30), $B-A=\xi>0$ can be written as:

$$\frac{D}{T^2/4\pi^2M^2C}-\frac{H}{Pr_2^2/4MC}=\xi>0. \tag{48}$$

Hence, the relation between the Poynting effect D and the axial force–twist effect H in a bilayered cylinder is concisely captured by Eq. (48). For a homogeneous cylinder of radius $r_2=R$, Eq. (48) reduces to:

$$\frac{D}{T^2/4\pi^2R^6\mu^2}-\frac{H}{P/4\mu}=\frac{2\nu}{1+\nu}>0, \tag{49}$$

where $\nu=\lambda/(2\lambda+2\mu)$ is the Poisson ratio. Eq. (48) is a universal relation in the sense that whatever the layer elastic constants and the radii are, this relation always holds. Eq. (49) also shows that for a homogeneous solid this relation is

essentially influenced by $2\nu/(1+\nu)$, which varies between 0 and 2/3 for $0 < \nu < 0.5$. Several logical relations can be drawn from Eqs. (48) or (49), assuming that the axial loading P is tensile:

(a) If $D < 0$, then necessarily $H < 0$,
(b) If $H > 0$, then necessarily $D > 0$.
(c) If H and D have different signs, then necessarily $H < 0$ and $D > 0$, meaning that the state $H > 0$ and $D < 0$ will never exist.
It should be emphasized that the converses of (a) and (b) are not true, i.e., $H < 0$ does not necessarily imply $D < 0$, and $D > 0$ does not necessarily imply $H > 0$. A further observation is that the sign of H will change if the sign of P changes, as can be seen from Eq. (30). Thus for the case of compressive axial loading, the above three conclusions should be changed to:
(d) If $D < 0$, then necessarily $H > 0$,
(e) If $H < 0$, then necessarily $D > 0$.
(f) If H and D have the same sign, then necessarily $H > 0$ and $D > 0$.

3. Numerical results

The objective of the numerical study is to illustrate the relation between the Poynting effect and the axial force–twist effect, and to investigate the influence of the elasticity and geometric inhomogeneities on D and H.

The elastic constants for certain soft solids, i.e., poly(acrylic acid) or PAA gels, agar-gelatin gels and polystyrene, are used as reference values. These reference values are varied in order to study how the effects depend on the elastic constants. Further, the elastic constants of generic polymer models, as estimated by Wu and Kirchner (2010), are also used in the study. The materials with these constants varied from the reference values are termed "PAA gel-based", "agar gelatin-based", etc. The radius r_1 is varied from 0 to the radius r_2 of the outer boundary. The applied torque assumes a magnitude of $T = 1, 10, 100$ or 1000×10^{-9} kPa m^3. The applied tensile stress $P = 0.01, 0.1$ or 1 kPa. The cylinder has the length of $L = 0.01$ m and an outer radius of $r_2 = 0.002$ m. The elastic constants, the radii and the loadings are summarized in Table 1.

Table 1
Elastic, geometrical and loading parameters used in Figs. 2–9.

	Material 1 Material 2	λ_1 λ_2	μ_1 μ_2	m_1 m_2	n_1 n_2	r_1	r_2	L	T	P
Fig. 2	Agar-gelatin-based	1.8×10^5	8	-20×10^6	80 1000	1	2	10	1	0.1
Fig. 3 (a)	PAA gel-based PAA gel-based	60 60		−35.6 −35.6	−23.5 −23.5	1	2	10	1	0.1
Fig. 3 (b)	PAA gel-based PAA gel-based	 60	12.21	−35.6 −35.6	−23.5 −23.5	1	2	10	1	0.1
Fig. 4 (a)	PAA gel-based PAA gel-based	60 60		−35.6 −35.6	−23.5 −23.5	1.414	2	10	1	0.1
Fig. 4 (b)	PAA gel-based PAA gel-based	60 60		−35.6 −35.6	−23.5 −23.5	1.9	2	10	1	0.1
Fig. 5 (a) and (b)	Agar gelatin-based Agar gelatin-based	 2.25×10^6	8	−2000 −2000	80 80	1	2	10	10	0.1
Fig. 6 (a) and (b)	Agar gelatin-based Agar gelatin-based	2.25×10^6 2.25×10^6		-20×10^6 -20×10^6	80 80	1	2	10	1	0.1
Fig. 7(a) and (b)	Polymer-based Polymer-based	35.7 35.7	10.3	−35.6	−23.5 −23.5	1	2	10	10	0.01
Fig. 8 (a)	PAA gel-based PAA gel-based	60 60	10 7	−35.6 −35.6	−23.5 −23.5		2	10	1000	1
Fig. 8(b)	Polymer-based Agar gelatin-based	10 2.25×10^6	200 80	−42.67 -20×10^6	−23.5 80		2	10	1000	1
Fig. 9 (a)	Polymer-based Agar gelatin-based	100 2.25×10^6	20 4	−4267 -20×10^6	−23.5 80		2	10	100	0.1
Fig. 9(b)	Myocaridal core-based Endocardial sheath-based	32670 4067	3.3 7	−36000 −420	2 −4.6		2	10	1000	1

Note: poly(acrylic acid) = PAA.
Units: λ, μ, l, m, n (kPa); r_1, r_2, L (mm); T (10^{-9} kPa m^3= 1 mN mm); P (kPa = 1mN/mm^2).

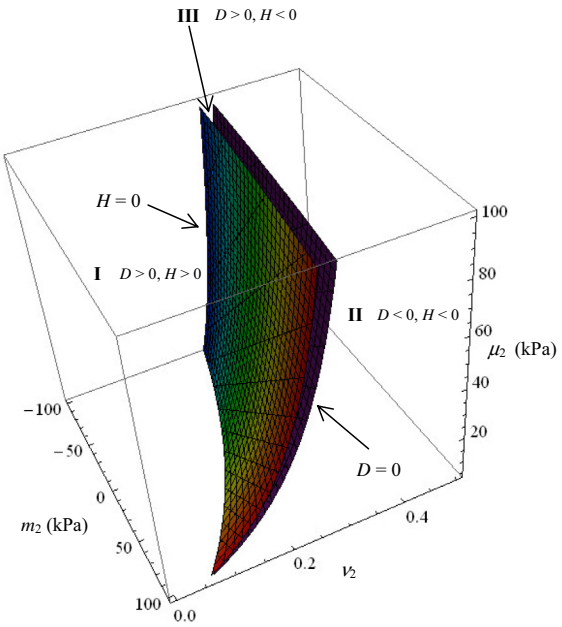

Fig. 2. The surfaces of $D = 0$ and $H = 0$ in the $\mu_2 - \nu_2 - m_2$ space for a bilayered cylinder. Only three regions are possible. Region I represents $D > 0$ and $H > 0$; Region II represents $D < 0$ and $H < 0$; Region III represents $D > 0$ and $H < 0$.

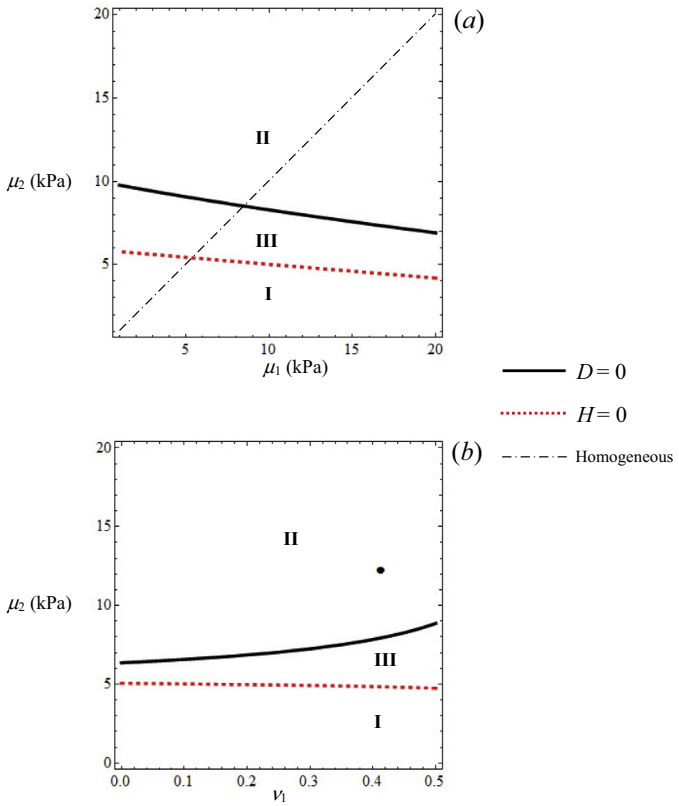

Fig. 3. Contours of the Poynting effect coefficient $D = 0$ (solid line) and axial force–twist effect coefficient $H = 0$ (dashed line) in (a) $\mu_1 - \mu_2$ space and (b) $\nu_1 - \mu_2$ space for a bilayered cylinder. The dot-dashed line and the dot represent homogeneous cylinders. The contours partition the space into three regions. Region I ($D > 0$ and $H > 0$); Region II ($D < 0$ and $H < 0$); Region III ($D > 0$ and $H < 0$).

3.1. Dependence of the sign of D and H on elastic constants

Layer elastic inhomogeneity is a key characteristic of a composite. This section investigates how it affects the relation between D and H. It confirms the inequality relations stated at the end of Section 2.4.

Fig. 2 plots the constant surfaces of $D = 0$ and $H = 0$ in the $\mu_2 - \nu_2 - m_2$ space for a soft composite cylinder subjected to combined torsional and axial loading. The other elastic constants, the loading and the geometrical parameters are fixed and listed in Table 1. Several observations can be made.

It can be seen that the space is partitioned into three regions: Region I represents $D > 0$ and $H > 0$, Region II $D < 0$ and $H < 0$, and Region III $D > 0$ and $H < 0$. The region of $D < 0$ and $H > 0$ does not exist. The relations between the two effects are in agreement with the logical relations (a) to (c) stated in Section 2.4. For Relation (a), Fig. 2 shows that negative Poynting effect ($D < 0$) implies negative axial force–twist effect ($H < 0$) as shown in Region II. Regions I and III are related to $D > 0$ only. Moreover, the converse is not true, i.e., negative axial force–twist effect ($H < 0$) does not imply negative Poynting effect ($D < 0$) necessarily, due to the existence of Regions II and III.

For Relation (b), Fig. 2 shows that a positive axial force–twist effect implies positive Poynting effect: $H > 0$ implies $D > 0$, as shown in Region I. Regions II and III are only associated with $H < 0$. The converse is again not true: $D > 0$ does not necessarily imply $H > 0$ due to the existence of Regions I and III. For Relation (c), which refers to the case when the two effects differ in sign, the Poynting effect must be positive and the axial force–twist effect must be negative, as shown in Region III. Region III is generally quite small, suggesting that only careful choices in the elastic constants can lead to differences in sign for the two effects.

Further observations can be made regarding how the effects depend on the elastic constants. Region II with $D < 0$ tends to occur when ν_2 is large, μ_2 is small and m_2 is positive. Many soft tissues are characterized as nearly incompressible with small shear modulus in the order of 10–100 kPa. Thus for soft tissues, they tend to have the negative Poynting effect. Janmey et al. (2007) found that many soft tissues generate a negative normal stress under shear. Wang and Wu (2014a) also showed that soft incompressible materials tend to demonstrate the negative Poynting effect. The new result here is that they also tend to show a negative axial force–twist effect. Finally, Fig. 2 shows that both the second- and third-order elastic parameters can be

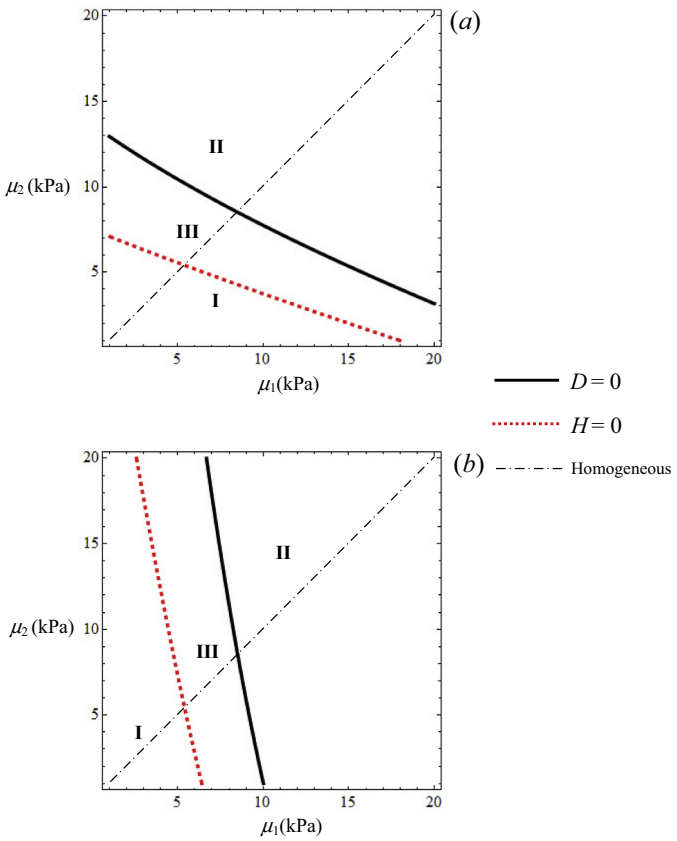

Fig. 4. Contours of the Poynting effect coefficient $D = 0$ (solid line) and axial force–twist effect coefficient $H = 0$ (dashed line) in $\mu_1 - \mu_2$ space with (a) $r_1 = 1.414$ mm and (b) $r_1 = 1.9$ mm for a bilayered cylinder. The dot-dashed line represents a homogeneous cylinder. The contours partition the space into three regions. Region I ($D > 0$ and $H > 0$); Region II ($D < 0$ and $H < 0$); Region III ($D > 0$ and $H < 0$).

used to adjust the sign of the Poynting and axial force–twist effects. This implies that soft solids can be accordingly designed with the desired nonlinear effects by manipulating the internal microstructure, e.g., the density of polymer chain links.

The influence of elastic inhomogeneity between the layers on the signs of D and H are studied in Fig. 3. This figure plots the $D = 0$ (solid line) and $H = 0$ (dashed line) contours in (a) $\mu_1 - \mu_2$ space and (b) $\nu_1 - \mu_2$ space for a bilayered cylinder. The other parameters are shown in Table 1. In Fig. 3(a), all the other elastic constants between the layers are the same. A homogeneous dot-dashed line, on which every point indicates a homogeneous cylinder, is drawn in Fig. 3(a). Several conclusions can be made based on Fig. 3.

First, only three regions (Regions I, II and III) exist. The region of $D < 0$ and $H > 0$ does not exist. Second, the contours are rather flat, which means that the effect of μ_2 is greater than μ_1 and ν_1. Thus the signs of D and H can be more easily controlled by adjusting μ_2. For this particular combination of materials, increasing μ_2 will turn both D and H negative. Third, the homogeneous line in Fig. 3(a) crosses all three regions. By adjusting the shear modulus μ of a homogeneous material, the sign of D and H can be altered. The dot in Fig. 3(b) also refers to the homogeneous case, which falls within Region II. Overall, Fig. 3 shows that the sign of the nonlinear effects is closely connected with the elastic inhomogeneity between the layers.

As the elastic-geometrical parameters A, B, C and M in Eqs. (31)–(34) show, the elastic and geometrical inhomogeneities are coupled in the form of quartic and sextic polynomials. This coupling is illustrated in Fig. 4, which plots the $D = 0$ (solid line) and $H = 0$ (dashed line) contours in $\mu_1 - \mu_2$ space for $r_1 = 1.414$ mm in (a) and $r_1 = 1.9$ mm in (b), respectively. As always, r_2 is fixed at 2 mm. All elastic constants and loadings are held fixed and given in Table 1. It can be observed that as r_1 increases from 1.414 to 1.9 mm, the slopes of the curves also increase. Thus, the influence of μ_2 is decreasing while that of μ_1 is increasing. In Fig. 4(a), the volumes of the two materials are the same. The influence of the two materials on the sign of D and H is comparable, with the effect of μ_2 slightly larger than that of μ_1. In Fig. 4(b), the signs of D and H are largely determined by μ_1, i.e., they can be more readily changed by adjusting μ_1 than by μ_2. It can be concluded that the combination of geometrical and elastic constants plays an important role in determining the sign of D and H. It is also noted that the reduced coefficients C_D and C_H will ensure identical sign and strength of the Poynting effect and the axial force–twist effect, respectively.

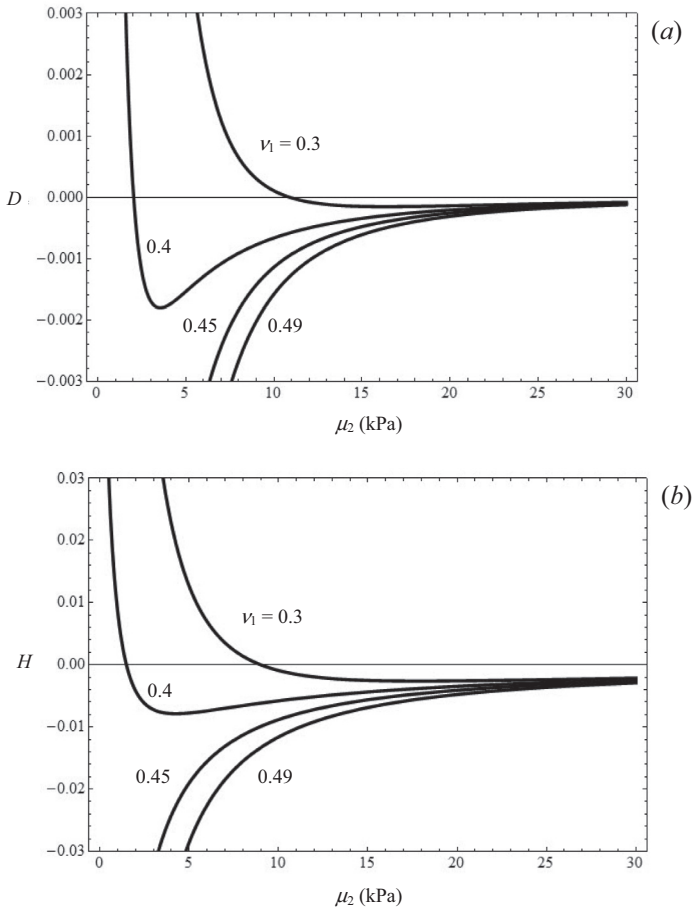

Fig. 5. Dependence of (a) D and (b) H on the shear modulus μ_2 for different Poisson ratios $\nu_1 = 0.3, 0.4, 0.45$ and 0.49 for a bilayered cylinder.

3.2. Influence of layer inhomogeneity on the magnitudes of D and H

As expected, the second- and third-order elastic constants can influence not only the sign but also the magnitude of D and H. Fig. 5 shows how the linear elastic constants μ_2 and ν_1 affect D and H. Here D and H are plotted against μ_2 for $\nu_1 = 0.3$, 0.4, 0.45 and 0.49 in Fig. 5(a) and (b), respectively. The other elastic parameters, the loadings and the cylinder radii are given in Table 1. Several observations can be made.

The signs and magnitudes of D and H can change quite drastically with μ_2. For $\nu_1 = 0.3$ and 0.4, both D and H change from negative to positive with a decreasing μ_2. However, for $\nu_1 = 0.45$ and 0.49, D and H are always negative. This again suggests that for nearly incompressible materials, D and H tend to be negative (in general, other elastic constants may also play a role). Furthermore, extrema are evidently present as the second-order elastic constants evolve. For example, a negative maximum of D is obtained at $\mu_2 \approx 3.55$ kPa and $\nu_1 = 0.4$. Similarly, a negative maximum of H is obtained at $\mu_2 \approx 4.24$ kPa and $\nu_1 = 0.4$. In the current example, H is of the order of 10^{-2}. Since H represents the ratio of the second-order to first-order twist, the second-order twist arising from the axial load application is not an insignificant part of the twist due to the torsion. This additional twist is also proportional to the axial load. Finally, the behavior at limiting values of μ_2 is noteworthy. As $\mu_2 \to \infty$, D and H will become zero. This is expected as the shear modulus of Layer 2 becomes infinitely large and it becomes increasingly difficult to stretch and twist the cylinder. As $\mu_2 \to 0$, D and H will tend to some finite values, since at the very minimum Layer 1 will continue to exhibit the Poynting and axial force–twist effects.

To study the elastic inhomogeneity more explicitly, Fig. 6 plots the dependence of D and H on μ_2 for different elastic inhomogeneity ratios $\alpha = \mu_1/\mu_2 = 0.1$, 1, 10 and 100. All the other elastic constants are the same for the two layers and are given in Table 1. The $\alpha = 1$ curve represents a homogeneous cylinder. For a homogeneous cylinder, D and H change from negative to positive as the shear modulus μ_2 increases. Interestingly, this remains true even if α changes to 0.1 or 100. Negative D and H are achieved at small μ_2. A second observation is that a positive extremum exists for each curve. The magnitude of the positive extremum decreases as α increases. The corresponding value of μ_2 at which the extremum occurs also becomes smaller (less than 10 kPa). These results can be made use of in a composite design. If the Layer 2 material is constrained to have a particular value of μ_2, and if large positive D and H are desired, then a small α is preferred. Or, if a certain minimum D or H is

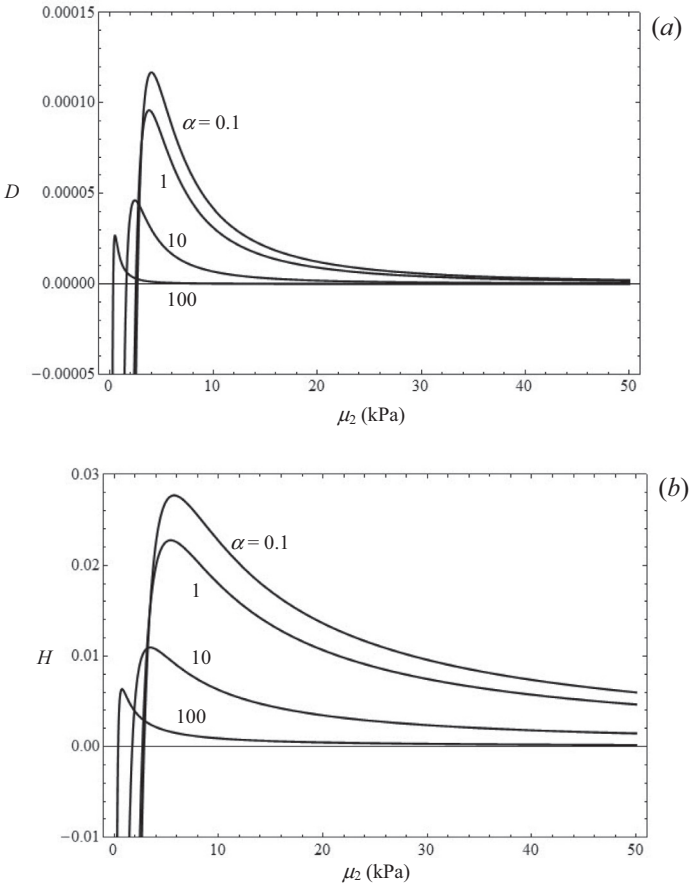

Fig. 6. Dependence of (a) D and (b) H on the shear modulus μ_2 for different inhomogeneity ratios $\alpha = \mu_1/\mu_2 = 0.1$, 1, 10 and 100.

required, a horizontal line can be drawn across the figure at that minimum value, which will delimit the appropriate boundary values of μ_1 and μ_2.

Fig. 7 illustrates how the nonlinear elastic constant m_2 can also significantly influence D and H. The dependence of D and H on μ_2 is plotted for $m_2 = \pm 2 \times 10^5, \pm 2 \times 10^4$ and 0 kPa. The other parameters are given in Table 1. As before, increasing μ_2 will decrease the magnitudes of D and H. Second, both D and H are positive for negative m_2 and negative for positive m_2. The effects are almost zero when $m_2 = 0$. Changing the sign of m_2 will basically reverse the sign of both D and H. Third, increasing the magnitude of m_2 will also increase the magnitudes of D and H. The magnitude can reach the order of 10^{-3} to 10^{-1} when μ_2 is small. The key result is therefore that the nonlinear effects can be amplified or reduced not only by second-order but also third-order elastic constants.

3.3. Dependence of D and H on geometric inhomogeneity

It is unclear how geometric inhomogeneity can affect the magnitude and sign of D and H. Figs. 8(a), (b) and 9(a), (b) plot D and H versus the interface position r_1, which changes from 0 to r_2, for four different bilayered compositions, respectively. The two ends of each curve represent homogeneous cylinders. When $r_1 = 0$, the cylinder is homogenous and composed entirely of Material 2. When $r_1 = r_2$, the cylinder contains only Material 1. The change from r_1 to r_2 can be described as an evolution of geometrical inhomogeneity. The curves in the figures essentially represent rational functions of polynomials; D for example is the ratio of a sixth-order polynomial over a twelfth-order polynomial.

It can be seen from the figures that both D and H can change from positive to negative, or remain positive or negative, when r_1 changes. The curves exhibit complex behavior with could at times be counter-intuitive. For instance, Fig. 8(b) shows that a composite consisting of Material 2 exhibiting a positive effect (both Poynting and axial force–twist) and a Material 1 exhibiting a negative effect may have this effect nullified if the interface position falls on $r_1 \sim 0.00187$ m. Also, extrema may exist while changing r_1 as shown in Fig. 9. This means an amplification effect arises, in which the magnitude of D and H of a composite may be larger than that of a homogeneous solid composed of either of its constituents. Fig. 9(b) shows, for

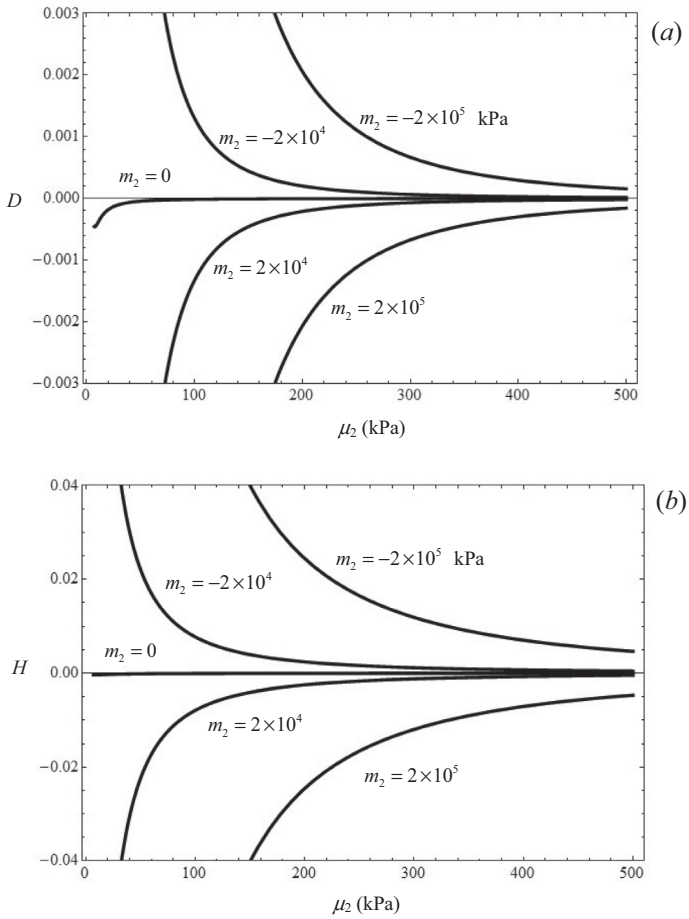

Fig. 7. Dependence of (a) D and (b) H on the shear modulus μ_2 for $m_2 = -2 \times 10^5,\ -2 \times 10^4,\ 0,\ 2 \times 10^4, 2 \times 10^5$ kPa.

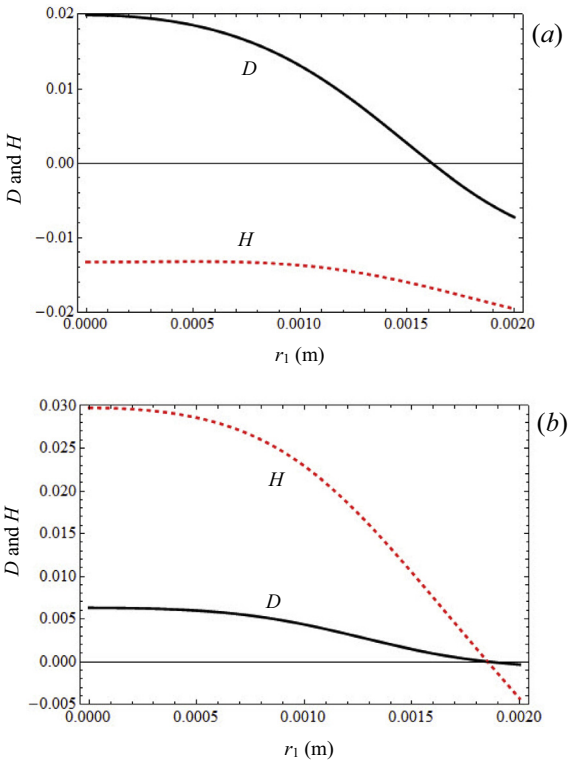

Fig. 8. Dependence of D (solid line) and H (dashed line) on the interface position r_1 for a bilayered cylinder of material compositions in the form Layer 1/Layer 2: (a) PAA gel-based/PAA gel-based, (b) polymer-based/agar gelatin-based.

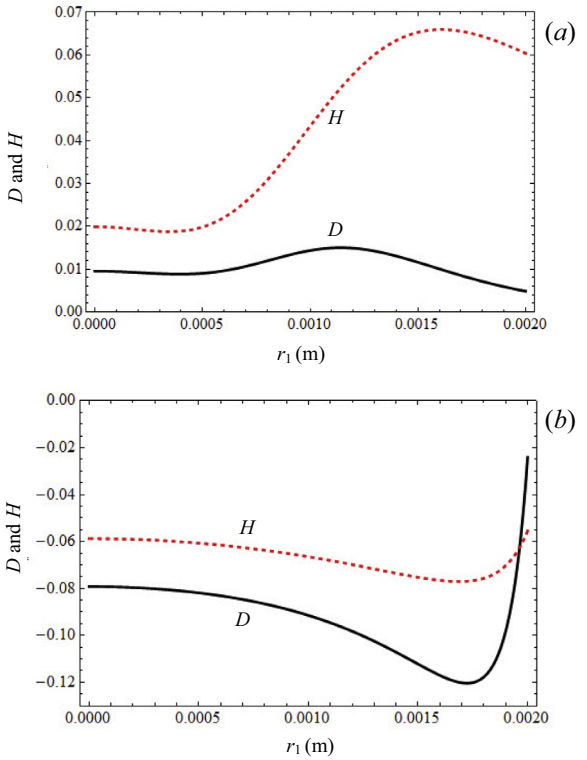

Fig. 9. Dependence of D (solid line) and H (dashed line) on the interface position r_1 for a bilayered cylinder of material compositions in the form Layer 1/Layer 2: (a) polymer-based/agar gelatin-based, (b) myocardial-based/endocardial-based.

instance, that $D \sim -0.08$ at $r_1 = 0$ m, $D \sim -0.025$ at $r_1 = r_2 = 0.002$ m, but a negative maximum $D \sim -0.12$ occurs at $r_1 = 0.00172$ m. Whether the nonlinear effect is amplified or reduced depends on the specific elastic inhomogeneity. It can be concluded that the interface position is also a key parameter in determining D and H.

4. Discussion

This work explores the relations between two nonlinear effects, the Poynting effect and the axial force–twist effect, in a bilayered cylinder. It has practical significance due to the ubiquitous presence of axial and torsional loadings in both man-made and living structures, many of which are composites. It is also of importance because the effects are not negligibly small compared to the first-order displacements and rotations. The importance of the Poynting effect is well-recognized by many researchers (Destrade & Saccomandi, 2010; Horgan & Murphy, 2011, 2012; Janmey et al., 2007; Mihai & Goriely, 2011, 2013; Misra et al., 2010; Storm et al., 2005; Wang & Wu, 2014a, 2014b; Wu & Kirchner, 2010; Zubov, 2001).

Associated with the Poynting effect are second-order normal stresses which arise when a block is sheared. Although not explicitly presented here, associated with the axial force–twist effect is an additional second-order shear stress (as well as the normal stresses) which also arises when a block undergoes generalized shear (Wang & Wu, 2014b). In generalized shear, the imposed shear displacement in a given direction is neither uniform nor restricted to be a linear function of the height variable. The second-order stresses exist in association with the imposed deformation gradients. These stresses may not be negligible and may therefore affect mechanical and biological functions.

The size dependence of the effects may also play a role in applications. According to Eqs. (45) and (46), the Poynting effect is more important at small than at large cylinder sizes, while the reverse is true for the axial force–twist effect. There exists a difference of three orders of magnitude between the dependences of these effects on size.

The logical relations between the Poynting and axial force–twist effects may be used as predictive tools during design considerations. For instance, many soft near-incompressible materials with low shear modulus and high Poisson ratio are known to exhibit the negative Poynting effect (Janmey et al., 2007; Storm et al., 2005). Then by Relation (a), these materials will also exhibit a negative axial force–twist effect under tension–torsion. Hence, under tension–torsion these materials will twist less than if they were to be subjected to torsion alone. However, by Relation (d) under compression and torsion, they will twist more compared to under torsion alone. Furthermore, note that none of the relations (a)–(f) are stipulated with the precondition $D > 0$. This means that if a material exhibits the positive Poynting effect, the sign of the axial force–twist effect cannot be inferred under tension–torsion or compression-torsion.

Besides the sign, the magnitude of the effects can be amplified, nullified or reduced depending on the applications. By Eqs. (25) and (30), the elastic constants and the interface position can be chosen to achieve the desired behavior. If there are restrictions to the selection of materials due to other considerations, the composite structure can be advantageously employed for the purpose, as the interface position has a strong influence on the effects.

Generalization of the model to multiple layers can be easily achieved in principle. This involves the imposition of interface conditions between the various contacting layers. However, the analytical expressions are expected to be complicated, as the number of elastic constants and radii increases considerably.

Finally, the theoretical results here may be complemented in the future by experimental studies. In particular, the following can be explored: measurement of the effects in a bilayered composite, variation of the effects with elastic constants and composite structure, and dependence of the effects on cylinder radius. Confirmation of the relations presented in this paper may also be carried out.

5. Conclusions

In this work, we presented a detailed investigation into the relations between two nonlinear effects, the Poynting effect and the axial force–twist effect, in a bilayered cylinder subjected to axial and torsional loading. The solutions pertaining to these effects are based on second-order elasticity. The dependence of these effects on the elastic and geometric inhomogeneities is emphasized. The key results may be summarized as follows.

First, both of these effects can be positive or negative. Second, only three possible combinations of states exist: both positive, both negative, or the Poynting effect is positive and the axial force–twist effect is negative (under tension–torsion). Third, logical relations exist between these effects. Under tension–torsion, if $D < 0$, then $H < 0$; if $H > 0$, then $D > 0$; and if D and H differ in sign, then $H < 0$ and $D > 0$. Fourth, a reduced parameter C_D which is the ratio of polynomials uniquely connects the Poynting effect to the square of the torsional load, and likewise another reduced parameter C_H connects the axial force–twist effect to the axial load. These reduced parameters of the elastic constants and the cylinder radii (10 parameters in total) alone capture the dependence of the nonlinear effects on the elastic and geometric inhomogeneities. Lastly, the inhomogeneities exert a strong influence on the effects. Changing either the second-order or third-order elastic constants can change the sign and magnitude of the effects. Similarly, changing the interface position will lead to such changes. A noteworthy result is the possible amplification of these effects when a composite is constructed from two homogeneous materials.

These results are significant in practical applications because they offer multiple options on materials and composite structure selection to achieve the targeted functions, such as the design of a biocomposite to exhibit a specific combination of signs and strengths for the Poynting and axial force–twist effects.

References

Destrade, M., & Saccomandi, G. (2010). On the rectilinear shear of compressible and incompressible elastic slabs. *International Journal of Engineering Science, 48*, 1202–1211.

Facca, S., Cortez, C., Mendoza-Palomares, C., Messadeq, N., Dierich, A., Johnston, A. P. R., et al (2010). Active multilayered capsules for in vivo bone formation. *Proceedings of the National Academy of Sciences of the United States of America, 107*, 3406–3411.

Horgan, C. O., & Murphy, J. G. (2011). Simple shearing of soft biological tissues. *Proceedings of the Royal Society a-Mathematical Physical and Engineering Sciences, 467*, 760–777.

Horgan, C. O., & Murphy, J. G. (2012). On the modeling of extension-torsion experimental data for transversely isotropic biological soft tissues. *Journal of Elasticity, 108*, 179–191.

Janmey, P. A., Mccormick, M. E., Rammensee, S., Leight, J. L., Georges, P. C., & Mackintosh, F. C. (2007). Negative normal stress in semiflexible biopolymer gels. *Nature Materials, 6*, 48–51.

Lenoe, E., Heller, R., & Freudenthal, A. (1965). Viscoelastic behavior of a filled elastomer in the linear and nonlinear range. *Transactions of The Society of Rheology, 9*(1957–1977), 77–102.

Murnaghan, F. D. (1951). *Finite deformation of an elastic solid*. New York: John Wiley.

Mihai, L. A., & Goriely, A. (2011). Positive or negative Poynting effect? The role of adscititious inequalities in hyperelastic materials. *Proceedings of the Royal Society A: Mathematical, Physical and Engineering Science*. rspa20110281.

Mihai, L. A., & Goriely, A. (2013). Numerical simulation of shear and the Poynting effects by the finite element method: An application of the generalised empirical inequalities in non-linear elasticity. *International Journal of Non-Linear Mechanics, 49*, 1–14.

Misra, S., Ramesh, K. T., & Okamura, A. M. (2010). Modelling of non-linear elastic tissues for surgical simulation. *Computer Methods in Biomechanics and Biomedical Engineering, 13*, 811–818.

Poynting, J. (1909). On pressure perpendicular to the shear planes in finite pure shears, and on the lengthening of loaded wires when twisted. *Proceedings of the Royal Society of London. Series A, Containing Papers of a Mathematical and Physical Character, 82*, 546–559.

Poynting, J. H. (1912). On the changes in the dimensions of a steel wire when twisted, and on the pressure of distortional waves in steel. *Proceedings of the Royal Society of London Series A, 86*, 534–561.

Stella, J. A., & Sacks, M. S. (2007). On the biaxial mechanical properties of the layers of the aortic valve leaflet. *Journal of Biomechanical Engineering-Transactions of the ASME, 129*, 757–766.

Storm, C., Pastore, J. J., MacKintosh, F. C., Lubensky, T. C., & Janmey, P. A. (2005). Nonlinear elasticity in biological gels. *Nature, 435*, 191–194.

Volokh, K. Y. (2006). Lagrangian equilibrium equations in cylindrical and spherical coordinates. *Cmc-Computers Materials & Continua, 3*, 37–42.

Wang, D., & Wu, M. S. (2014a). Poynting and axial force–twist effects in nonlinear elastic mono- and bi-layered cylinders: Torsion, axial and combined loadings. *International Journal of Solids and Structures, 51*, 1003–1019.

Wang, D., & Wu, M. S. (2014b). Generalized shear of a soft rectangular block. *Journal of the Mechanics and Physics of Solids, 70*, 297–313.

Wu, M. S., & Kirchner, H. O. K. (2010). Nonlinear elasticity modeling of biogels. *Journal of the Mechanics and Physics of Solids, 58*, 300–310.

Zubov, L. M. (2001). Direct and inverse Poynting effects in elastic cylinders. *Doklady Physics, 46*(9), 675–677.